

Institute for Hadronic Structure and Fundamental Symmetries  
School of Natural Sciences  
Technical University of Munich

# Development of FPGA frontend electronics of the scintillating fiber hodoscope of AMBER at CERN

**Tim Maehrholz**

Bachelor's Thesis

Supervisor:

**Prof. Dr.**

Chair of

Second Examiner:

PD Dr.

January 2025



---

## Abstract

---

Here will be my abstract for thesis Thesis template from the ZNN, updated for Biblatex and Biber.



<b>1. Introduction</b>	<b>1</b>
<b>2. Theoretical concepts and overview of AMBER</b>	<b>3</b>
2.1. Measurment of the charge radius of the proton (PRM) . . . . .	3
2.1.1. Previous measurements of the proton radius . . . . .	3
2.1.2. Elastic scattering of muons on protons . . . . .	3
2.2. General setup for PRM at AMBER. . . . .	4
2.2.1. Detectors for PRM . . . . .	4
2.2.2. Scintillating fiber hodoscope(SFH) . . . . .	7
2.3. Field Programmable Gate Arrays (FPGAs) . . . . .	8
<b>3. Frontend electronic of the scintillating fiber hodoscope</b>	<b>9</b>
3.1. Overview of the frontend electronics . . . . .	9
3.1.1. Proccesing of the SFH signal . . . . .	10
3.1.2. The analog frontend electronics (FEE) PCB . . . . .	10
3.1.3. The iFTDC . . . . .	11
3.2. The Citiroc1A ASIC . . . . .	11
3.2.1. Signal proccesing of the Citiroc1A . . . . .	12
3.3. Configuration of the Citiroc1A . . . . .	13
3.3.1. The slow control register . . . . .	13
3.3.2. The probe register . . . . .	15
<b>4. Development of the FPGA firmware for CITIROC ASIC</b>	<b>17</b>
<b>5. Results</b>	<b>19</b>

---

<b>6. Discussion</b>	<b>21</b>
<b>7. Conclusion and Outlook</b>	<b>23</b>
7.1. Conclusion . . . . .	23
7.2. Outlook . . . . .	23
<b>Appendix A. Code</b>	<b>25</b>

# CHAPTER 1

---

## Introduction

---

"Nature will reveal its secrets, but only if we ask the right questions." [Werner Heisenberg]  
Progress in particle physics has always been driven by the desire to understand the fundamental building blocks of our universe.

Our current best theory for the innnerworkings of our world, the standart model of particle physics shows us, that the matter we see around us is mostly made up of down and up quarks and electrons. Combinations of these quarks, held together by the strong nuclear force form the proton and neutron,the nuclei of the atoms that make up the matter of the everyday world. Eventhough the Proton was discovered over a hundred years ago by Ernest Rutherford[8], it is still not fully understood.

Since the proton, unlike the electron is a composite particle, it follows that it has an internal structure. The semantic meaning of size in the realm of particеле physics is not as straight forward as in the macroscopic world.An answer to the question, what is the size of the proton can be given by looking at the charge distribution of the proton, which defines the charge radius of the proton.

The proton radius measurment at AMBER at CERN aims to reselove a discrepency between the charge radius of the proton as measured by the Lamb shift in muonic and ordinary hydrogen and the electron-proton scattering experiments, the so called proton radius puzzel.

To achieve this, the PRM experiment will measure the cross section of elastic scattering of muons on protons. The scintillating fiber hodoscope is a key component of the PRM experiment, as it provides crucial time measuments of the incoming and scattered mouns, needed for the measurment of the proton radius[1].

This thesis will focus on the development of the FPGA driven frontend electronics of the scintillating fiber hodoscope for the proton radius measurment at AMBER at CERN, especially on the development of the FPGA firmware required for the control of the Citiroc1A ASIC, a part of the readout and trigger electronic.



---

### Theoretical concepts and overview of AMBER

---

#### **2.1. Measurment of the charge radius of the proton (PRM)**

The proton is a baryon, a composite particle made up of one down quark and two up quarks. From this follows that the proton is not a point particle, but has an internal sturucture.

The internal structure can be discribed by the structure functions of the proton, the electric and magnetic form factors  $G_E$  and  $G_M$  [1].

##### **2.1.1. Previous measurements of the proton radius**

The charge radius of the proton has been massured several times before with different methods. The two premier methods are electron proton scattering experiments and the Lamb shift in muonic and ordinary hydrogen. The results of these measurements differ by five standard deviations as shown in figure 2.1, this has given rise to the so called proton radius puzzle [1].

##### **2.1.2. Elastic scattering of muons on protons**

The AMBER PRM experiment at CERN aims to reslove the proton radius puzzle, by measuring the elastic scattering of muons on protons. The first order cross section,taking

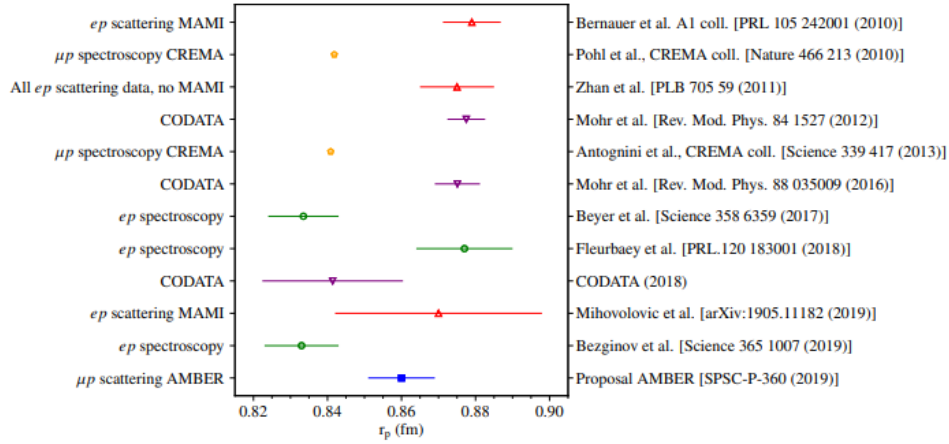


Figure 2.1.: Previous measurements of the proton radius from electron proton scattering experiments and the Lamb shift in muonic and ordinary hydrogen, the measurements differ from each other by five standard deviations. [1]

into account only interactions where one virtual photon was exchanged, for the elastic scattering of muons on a proton target is [2]

$$\frac{d\sigma}{dQ^2} = \frac{\pi\alpha^2}{Q^4 m_p^2 p_\mu^2} \left[ (G_E^2 + \tau G_M^2) \frac{4E_\mu^2 m_p^2 - Q^2(s - m_\mu^2)}{1 + \tau} - G_M^2 \frac{2m_\mu^2 Q^2 - Q^4}{2} \right] \quad (2.1)$$

with  $Q^2 = -q^2$  the squared transferred four-momentum,  $\tau = Q^2/4m_p^2$ ,  $s = (p_\mu + p_p)^2$ ,  $G_E$  the electric form factor of the proton,  $G_M$  the magnetic form factor of the proton and  $\alpha$  the fine structure constant.

Through determining the form factor  $G_E$  for small  $Q^2$ , the charge radius of the Proton can be calculated with the following equation [2]

$$r_p^2 = -6 \left. \frac{dG_E}{dQ^2} \right|_{Q^2=0} \quad (2.2)$$

## 2.2. General setup for PRM at AMBER.

### 2.2.1. Detectors for PRM

To determine the magnetic  $G_M$  and electric form  $G_E$  factors of the proton and thus the charge radius of the Proton, the experimental cross section of the elastic scattering of muons on protons has to be measured.

The general setup of the PRM experiment, with focus on the new detectors needed for the proton radius measurement, is shown in figure 2.2.

## 2.2. General setup for PRM at AMBER.

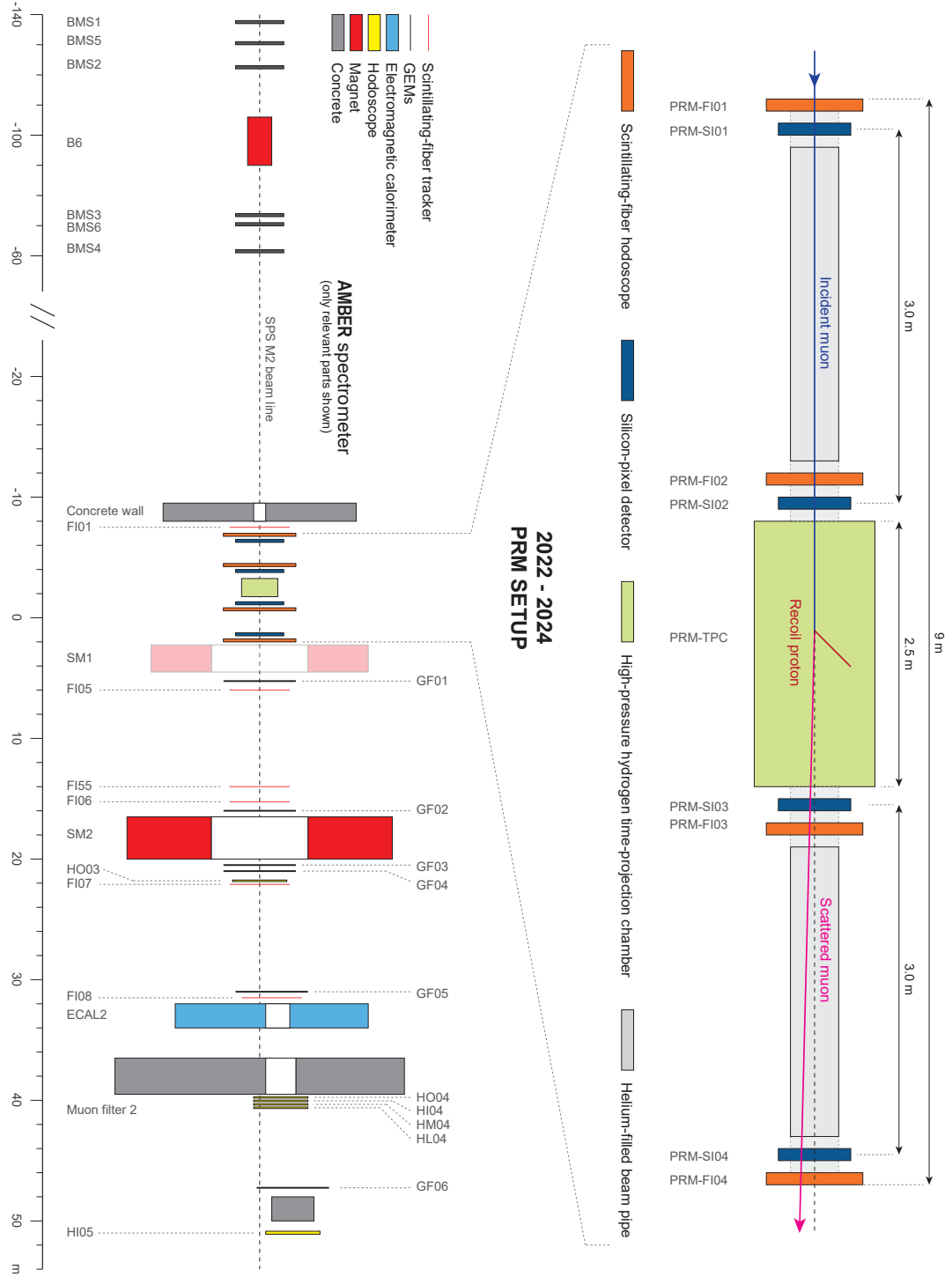


Figure 2.2.: General setup of the Amber experiment with new detectors for PRM. [5]

The incoming muon beam with an energy of 100 GeV[1] and an beam rate of  $2 \times 10^6$ [3] particles per second is scattered on a pressurized hydrogen gas target, located in the Time Projection Chamber (TPC), which also acts as the detector for the recoil path of

the scattered proton.

The reconstruction of the path of the muon is achieved through the usage of two detector types, combined into one unified tracking station (UTS) as shown in figure 2.3.

Each UTS consists of three layers of pixilized silicon detectors (ALPIDEs), for precises positional measurments (spacial resolution of about  $8\text{ }\mu\text{m}$  [6]) of the incoming and scattered muons, but lacking the time resolution( $5\text{ }\mu\text{s}$ [6]) required for the PRM experiment. For this reason each UTS includes a scintillating fiber hodoscope (SFH),the detector of intrest for this thesis, which provides the time precision( $300\text{ ps}$ [6]) for the measurment.

Four of these unified tracking stations, two before and two after the active target, are placed in the beamline as shown in 2.2. The measurment of the momentum of the scattered moun is done by existing COMPASS detectors located after the, for the PRM newly included, detectors[1].

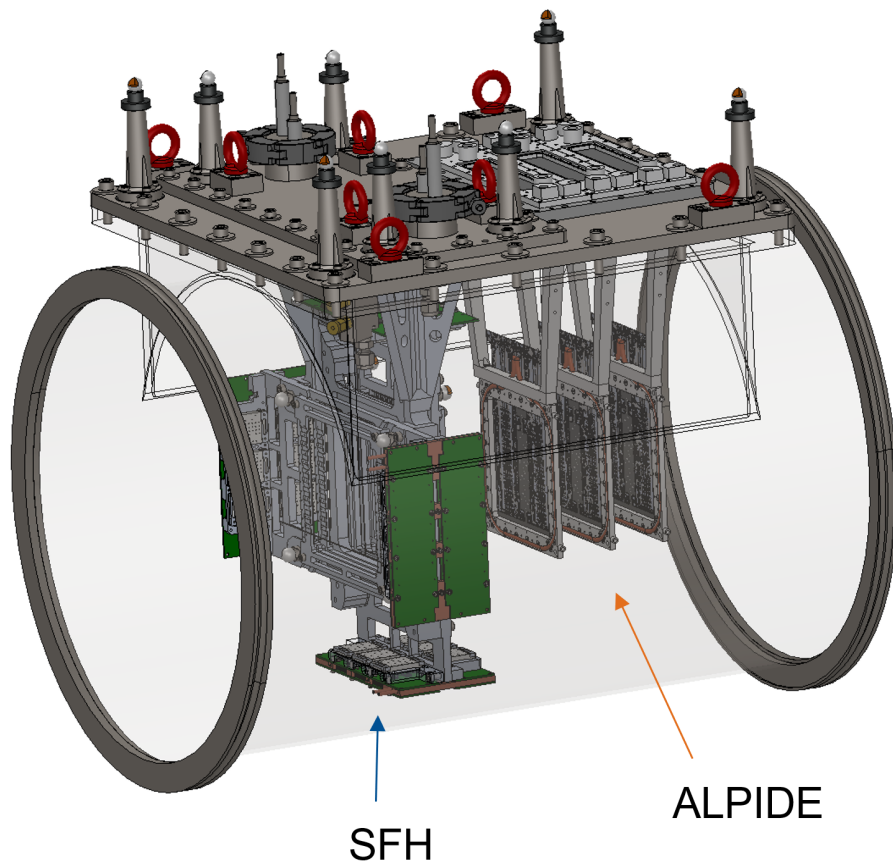


Figure 2.3.: Unified tracking station (UTS) with three layers of pixilized silicon detectors (ALPIDEs) and the scintillating fiber hodoscope (SFH). [5]

### 2.2.2. Scintillating fiber hodoscope(SFH)

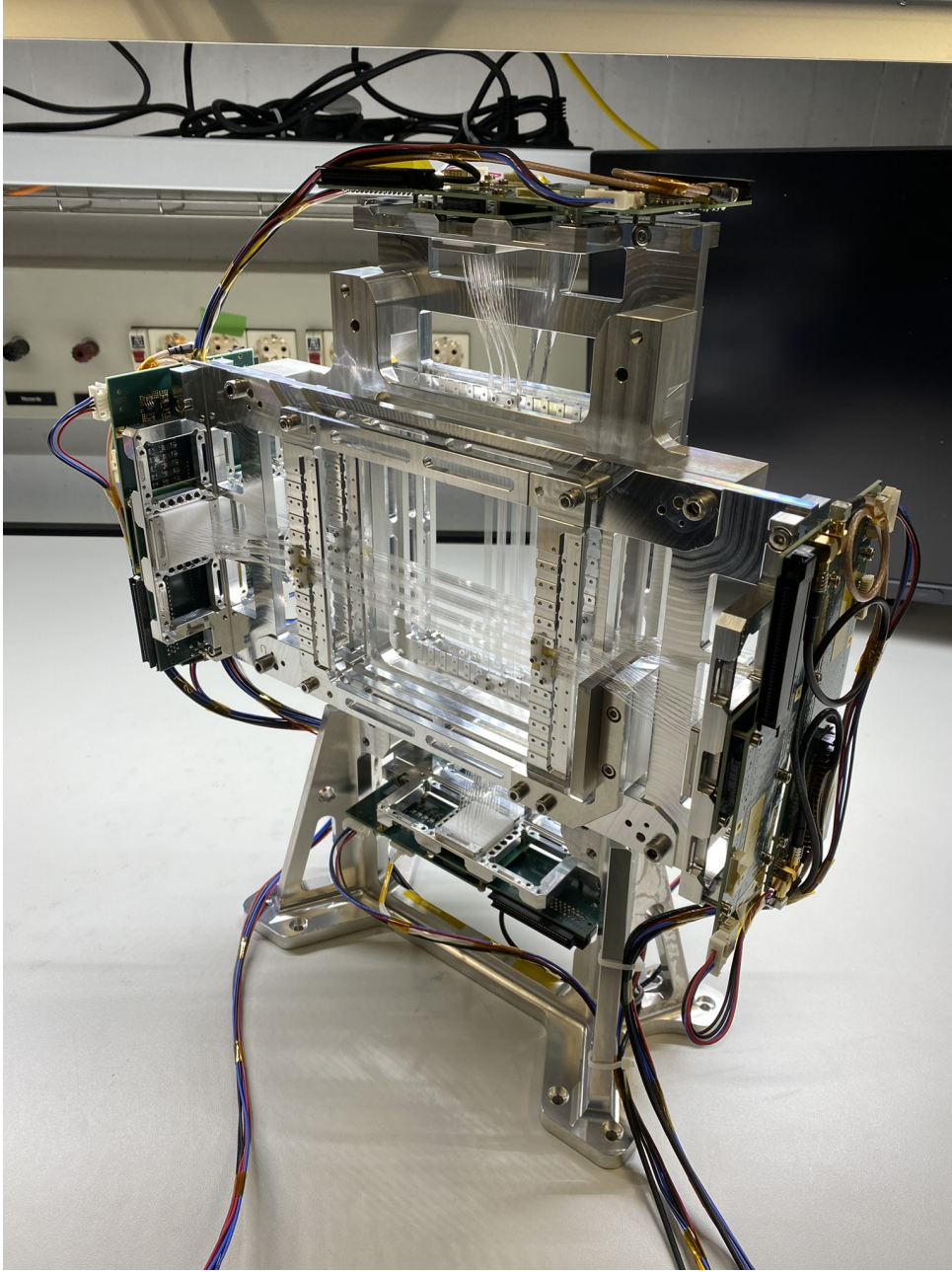


Figure 2.4.: Scintillating fiber hodoscope (SFH) with some of the scintillating fibers of the four layers installed. The frontend electronics are not attached.[5]

The scintillating fiber hodoscope shown in figure 2.4, the detector for which the FPGA driven frontend electronics are developed in this thesis, is used to measure the precise timing(300 ps[6]) of the incoming and scattered muons. Every SFH contains four layers of scintillating fibers, two in x and two in y direction. Each layer is made up of 192[6], 500  $\mu\text{m}$  thick[4] fibers, in total 768[6] fibers per SFH. When charged particles, muons in

this case, pass through a scintillating fiber they excite the scintillating material, which then emits photons. Both ends of every fiber are connected to a silicon photomultiplier (SiPM) which converts the photons into an electrical signal, that is then processed by the frontend electronics.

### **2.3. Field Programmable Gate Arrays (FPGAs)**

hallo [\[7\]](#)

## Frontend electronic of the scintillating fiber hodoscope

### 3.1. Overview of the frontend electronics

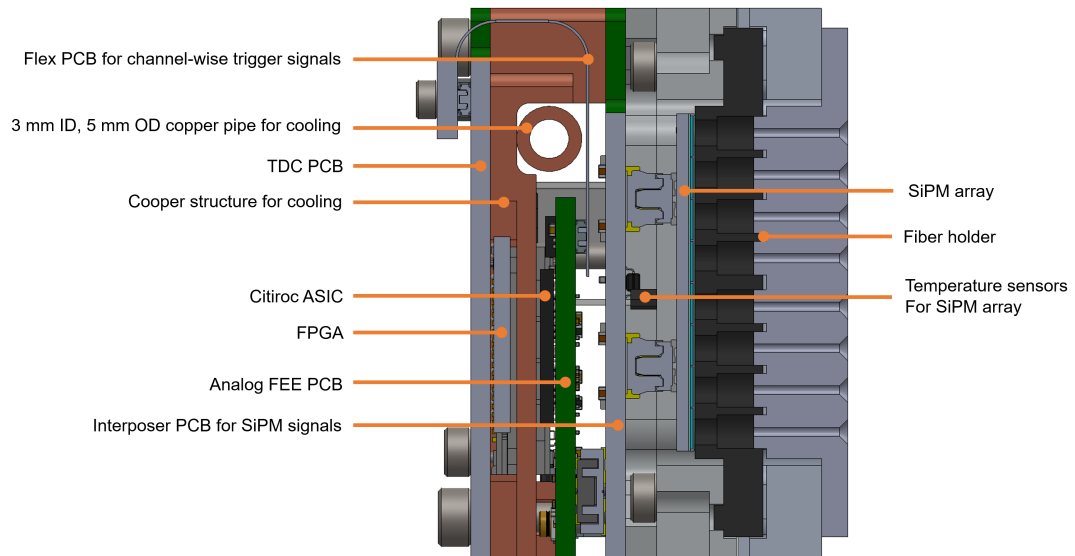


Figure 3.1.: Sideview of the frontend electronics that will be attached on the sides of the SFH, the fiber holders will be attached to the fibers. The SiPM arrays transform the incoming photons into electric signals, that are then transferred to the frontend electronics by the PCB interposer.[5]



### 3.1.1. Processing of the SFH signal

The frontend electronics of the scintillating fiber hodoscope process the signals from the scintillating fibers. They can be attached on all four sides of the SFH, as can be seen in figure 2.4. The fibers are connected to the fiber holders on both ends as shown in figure 3.1. There are in total 768[6] fibers per SFH. Since both ends produce an electric signal, a total of 1546 signals or 384 signals, for every attached electronics unit have to be processed.

The incoming photons are transformed into electric signals by the SiPM arrays. The SiPM signals are then transmitted to the analog frontend electronics (FEE) PCB by the interposer PCB also shown in figure 3.1.[5]

### 3.1.2. The analog frontend electronics (FEE) PCB

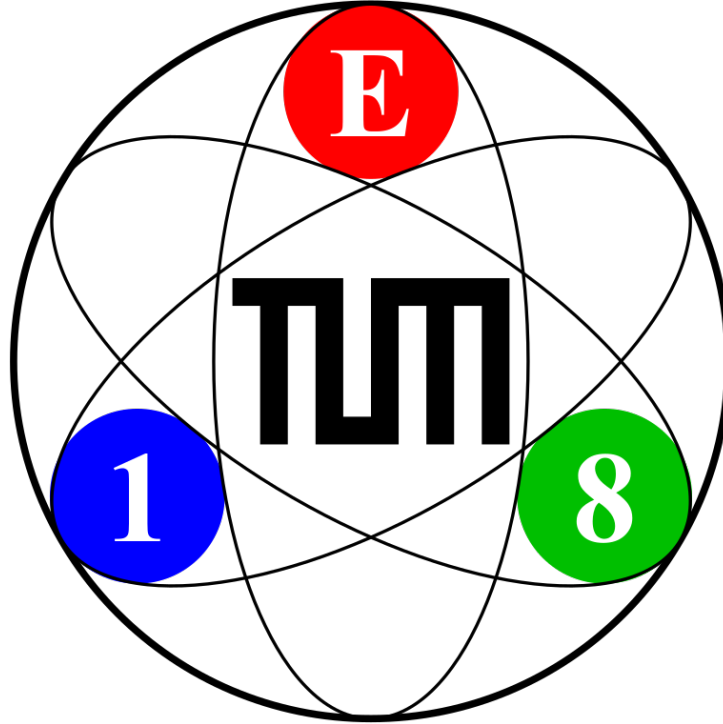


Figure 3.2.: The analog frontend electronics (FEE) PCB with the six Citiroc1A ASICs, on the left side the power supply is connected. The output of the Citiroc1A is transmitted to the iFTDC over three flex PCBs.[5]

The analog frontend electronics (FEE) PCB, shown in figure 3.2, together with the iFTDC form the heart of the frontend electronics. The FEE PCB incorporates six Citiroc1A ASICs, which are designed to amplify and process the signals from the SiPM arrays. Each Citiroc1A ASIC handles 32 signals. The output of the Citiroc1A is then transmitted to the iFTDC over three flex PCBs. The power supply is connected to the FEE PCB on



the left side as shown in 3.2. Two Citiroc1A ASICs are each controlled by one Artix-7 FPGA located on the iFTDC.[7]

### 3.1.3. The iFTDC

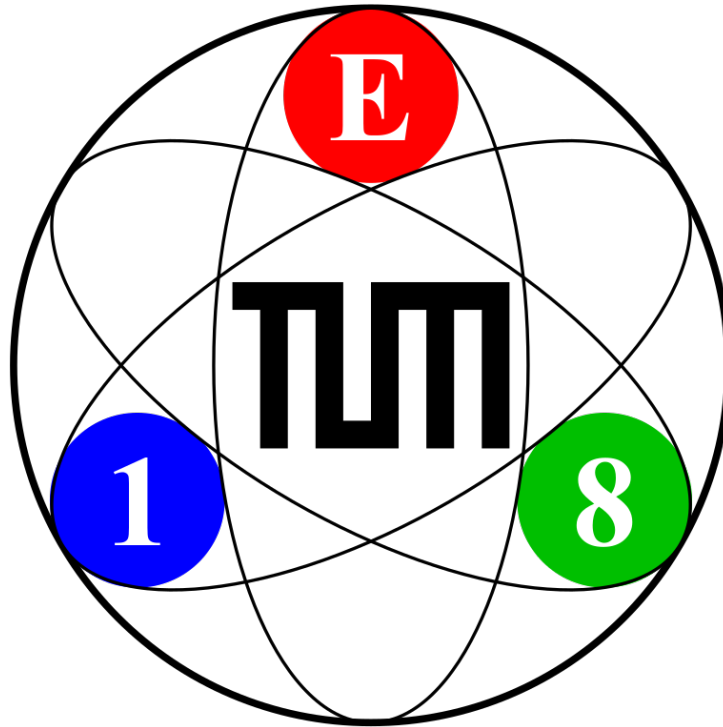


Figure 3.3.: The iFTDC with three Artix-7 FPGA, the three flex PCBs that connect the iFTDC with the FEE PCB and the power supply.[7]

The iFTDC, depicted in figure 3.3 is a FPGA based time-to-digital converter. It consists of three Artix-7 FPGA, who each control two Citiroc1A ASICs. The FPGA handles the readout as well as the configuration of the Citiroc1A ASICs[7].

INSERT: here stil hast to be includes how ethernet works how ipbus works and how jtag is implemented ans stuff analong this line

## 3.2. The Citiroc1A ASIC

The Citiroc1A ASIC is a frontend application-specific integrated circuit developed by Weeroc for the readout of SiPM detectors. It allows for the readout of 32 channels and is sensitive to  $\frac{1}{3}$  of a photoelectron.[9]

The Citiroc1A ASIC is controlled and readout by the Artix-7 FPGA on the iFTDC, each FPGA controlling two Citiroc1A ASICs.[7] The focus of this thesis is the development of

the FPGA firmware for the control of the Citiroc1A ASICs, but a provisional readout firmware for testing the configuration of the Citiroc1A will also be developed.

### 3.2.1. Signal processing of the Citiroc1A

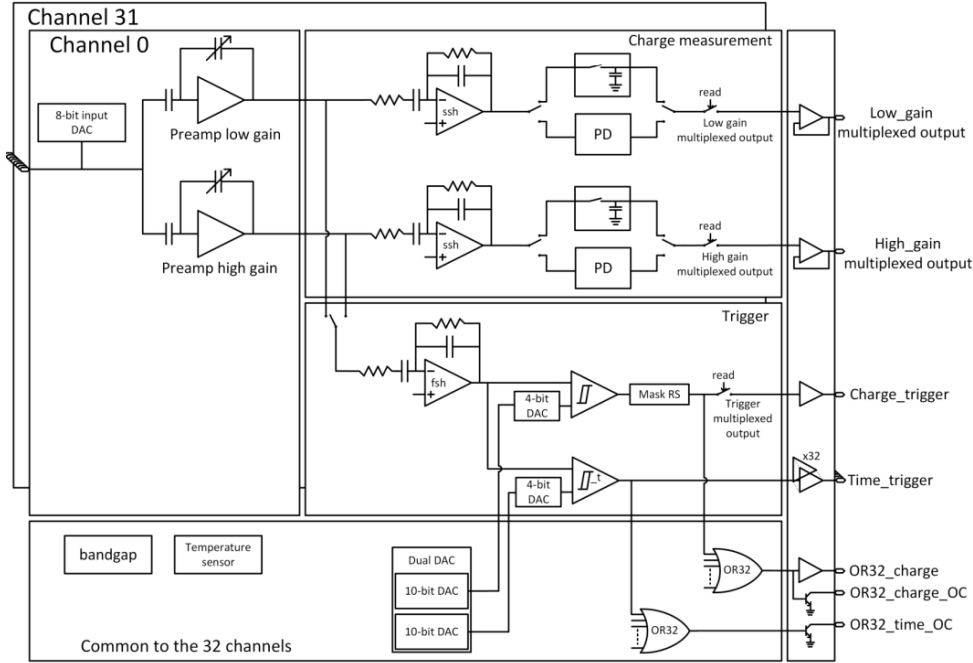


Figure 3.4.: General ASIC block scheme of the Citiroc1A. [9]

The general block scheme of the Citiroc1A is shown in figure 3.4.

The Citiroc1A allows for the fine tuning of the SiPM bias voltage for each channel via the 8-bit input DAC.

The input signals are amplified with a variable high or low gain, configurable for every channel as depicted in figure 3.5. The PRM experiment requires the maximal high gain of 62.[7]

The amplified signals are then shaped by either the slow (ssh) or fast shaper (fsh) as shown in figure 3.4. The fast shaper is used for the PRM experiment, since it has a 15 ns peaking time, which is needed for the time precision of the SFH.

The ASIC has two discriminators, the charge discriminator and the time discriminator. In this thesis we will only look at the time discriminator, since it provides the time information. The time discriminator threshold is adjustable via a 10 bit dac for all channels and an additional 4 bit dac for every individual channel as shown in figure 3.4 [9].

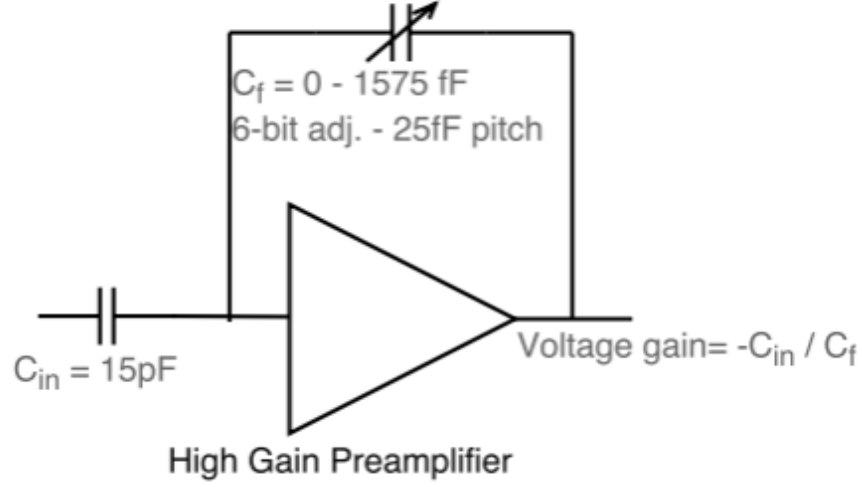


Figure 3.5.: High gain amplification of the Citiroc1A. The gain is adjustable from 0 to 1575 fF in 25 fF steps.[9]

### 3.3. Configuration of the Citiroc1A

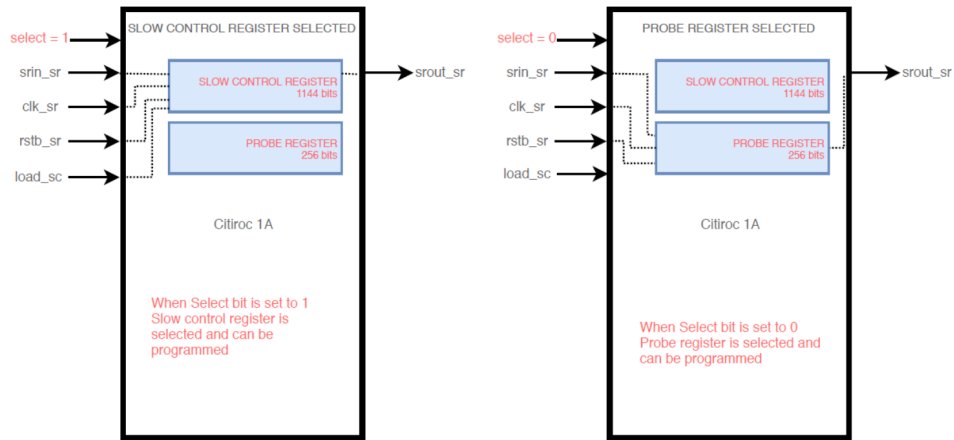


Figure 3.6.: BLABLABLUB[9]

The configuration of the Citiroc1A is achieved by the FPGA via the five signals shown in figure 3.6. The SELECT signal allows the choice between configuring the slow control, for SELECT = 1 or the probe register, for SELECT = 0.[9]

#### 3.3.1. The slow control register

The slow control register is used to set values for internal variables like the high gain for a channel or the time discriminator threshold. It also allows for the FPGA to turn

of specific stages of the Citiroc1A, like the slow shaper or the time discriminator. The register is 1144 bits long, a full list of all the register that can be set is shown in table 3.1.

Table 3.1.: Configurable registers of the slow control register[5]

Parameter	Bits	Default	Range	Description
<b>Channel Thresholds (Time)</b>				
ch_0	4	0	0	Channel-dependent 4-bit threshold for time discriminator.
...				Common 10-bit threshold (not detailed here).
ch_31	4	0		
<b>Channel Thresholds (Charge)</b>				
ch_0	4	0	128	Channel-dependent 4-bit threshold for charge discriminator.
...				Common 10-bit threshold (not detailed here).
ch_31	4	0		
<b>Discriminator Power</b>				
discriminator_charge_en	1	0	256	Enable charge discriminator.
discriminator_time_en	1	1		Enable time discriminator.
discriminator_latched_output	1	0	1	1: latched, 0: direct output.
<b>Amplifier and Shaper</b>				
high_gain_pp	1	0		High gain post-processing.
low_gain_en	1	0		Enable low gain path.
low_gain_slow_shaper_time_const	3	0	See table	Low-gain shaper time constant.
<b>Pre-Amplification</b>				
low_gain_weak_bias	1	0		0: normal bias, 1: weak bias.
ch_0_hg	6	62	619	High-gain preamp setting for ch_0.
ch_0_disable	1	0		1 disables preamp for ch_0.
<b>Threshold DACs</b>				
charge_dac_en	1	0	1103	Enable charge threshold DAC.
time_threshold	10			54V bias: 200 for 1 cell minimum, 250 for 2 cell minimum.
<b>Output and Debugging</b>				

*Continued on next page...*

**Table 3.1** Continued: Configurable registers of the slow control register[5]

Parameter	Bits	Default	Range	Description
digital_output_en	1	1		Enable digital multiplexed output.
trigger_polarity	1	0		0: positive (rising edge), 1: negative (falling edge).

### 3.3.2. The probe register

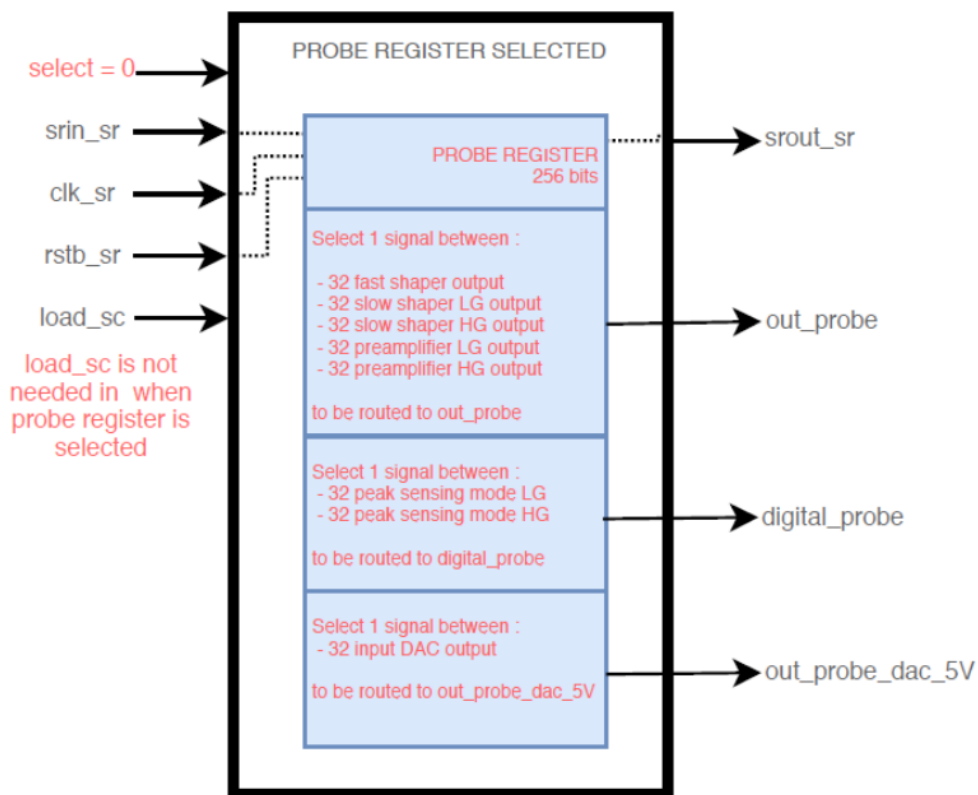


Figure 3.7.: BLABLABLUB[9]

The probe register is used for routing internal signals to several output pins for debugging purposes. Its functionality is illustrated in figure 3.7. The register consists of 256 bits and is written similarly to the slow control register, with the difference that the bits are directly written into the Citiroc1A without requiring a rising edge on `load_sc`.

The internal signals for each channel that can be routed to the output pins are shown in table 3.2.

Only one signal source can be routed to one output pin at a time, without potentially causing a short circuit.

Signal Source	Description	Output Pin
High and low gain preamplifier, slow and fast shapers	Outputs of preamplifiers and shapers	out_probe
PeakSensing_modeb_LG	Internal peak-sensing signal for low gain	digital_probe
PeakSensing_modeb_HG	Internal peak-sensing signal for high gain	digital_probe
Output of input DAC	DAC output voltage (5 V)	out_probe_dac_5_V

Table 3.2.: Internal signal routing to output pins for each channel.

## CHAPTER 4

---

### Development of the FPGA firmware for CITIROC ASIC

---

Here i describe the development of the FPGA firmware for the CITIROC ASIC.





## CHAPTER 5

---

### Results

---



## CHAPTER 6

---

Discussion

---

Discussion



## CHAPTER 7

---

### Conclusion and Outlook

---

#### **7.1. Conclusion**

Conclusion

#### **7.2. Outlook**

Outlook



## APPENDIX A

---

Code

---

```
1 this is code
```





---

## List of Figures

---

2.1.	Previous measurements of the proton radius from electron proton scattering experiments and the Lamb shift in muonic and ordinary hydrogen, the measurements differ from each other by five standard deviations. [1] . . .	4
2.2.	General setup of the Amber experiment with new detectors for PRM. [5] .	5
2.3.	Unified tracking station (UTS) with three layers of pixilized silicon detectors (ALPIDEs) and the scintillating fiber hodoscope (SFH). [5] . . . . .	6
2.4.	Scintillating fiber hodoscope (SFH) with some of the scintillating fibers of the four layres installed.The frontend electronics are not attached.[5] . . . .	7
3.1.	Sideview of the frontend electronics that will be attached on the sides of the SFH, the fiber holders will be attached to the fibers. The SiPM arrays transform the incoming photons into electric signals, that are then transferred to the frontend electronics by the PCB interposer.[5] . . . . .	9
3.2.	The analog frontend electronics (FEE) PCB with the six Citiroc1A ASICs, on the left side the power supply is connected.The output of the Citiroc1A is transmitted to the iFTDC over three flex PCBs.[5] . . . . .	10
3.3.	The iFTDC with three Artix-7 FPGA, the three flex PCBs that connect the iFTDC with the FEE PCB and the power supply.[7] . . . . .	11
3.4.	General ASIC block scheme of the Citiroc1A. [9] . . . . .	12
3.5.	High gain amplification of the Citiroc1A. The gain is adjustable from 0 to 1575 fF in 25 fF steps.[9] . . . . .	13
3.6.	BLABLABLUB[9] . . . . .	13
3.7.	BLABLABLUB[9] . . . . .	15



---

## Bibliography

---

- [1] B Adams et al. *COMPASS++/AMBER: Proposal for Measurements at the M2 beam line of the CERN SPS Phase-1: 2022-2024*. Tech. rep. Geneva: CERN, 2019. URL: <https://cds.cern.ch/record/2676885> (cit. on pp. 1, 3–6).
- [2] B. Adams et al. *Letter of Intent: A New QCD facility at the M2 beam line of the CERN SPS (COMPASS++/AMBER)*. 2019. arXiv: 1808.00848 [hep-ex]. URL: <https://arxiv.org/abs/1808.00848> (cit. on p. 4).
- [3] Maxim Alexeev et al. “Design and Testing of a new Tracking System for the Proton Charge Radius Measurement with the AMBER Experiment at CERN”. In: *PoS VERTEX2023* (2024), p. 049. DOI: 10.22323/1.448.0049 (cit. on p. 5).
- [4] The AMBER Collaboration. *AMBER Status Report 2024*. Tech. rep. Geneva: CERN, 2024. URL: <https://cds.cern.ch/record/2907624> (cit. on p. 7).
- [5] Karl Eichhorn. Private Communication. Nov. 2024 (cit. on pp. 5–7, 9, 10, 14, 15).
- [6] J M Friedrich and O Denisov. *AMBER Status Report 2022*. Tech. rep. Geneva: CERN, 2022. URL: <https://cds.cern.ch/record/2810822> (cit. on pp. 6, 7, 10).
- [7] Igor Konorov. Private Communication. Oct. 2024 (cit. on pp. 8, 11, 12).
- [8] Barrie M. Peake. “The discovery of the electron, proton, and neutron”. In: *Journal of Chemical Education* 66.9 (1989), p. 738. DOI: 10.1021/ed066p738 (cit. on p. 1).
- [9] Weeroc. *citiroc1a-datasheet-v2-53*. Dec. 2019. URL: <https://www.weeroc.com/~documents/products/citiroc-1a/citiroc1a-datasheet-v2-53/?layout=file> (cit. on pp. 11–13, 15).



---

## Acknowledgement

---

I want to thank:

**Tutor .**

**Professor .**



---

## Eidesstattliche Erklärung

---

Ich versichere hiermit an Eides statt, dass ich die von mir eingereichte Arbeit bzw. die von mir namentlich gekennzeichneten Teile selbständig verfasst und ausschließlich die angegebenen Hilfsmittel benutzt habe. Die Arbeit wurde bisher in gleicher oder ähnlicher Form in keiner anderen Prüfungsbehörde vorgelegt und auch noch nicht veröffentlicht.

Ort, Datum

Unterschrift